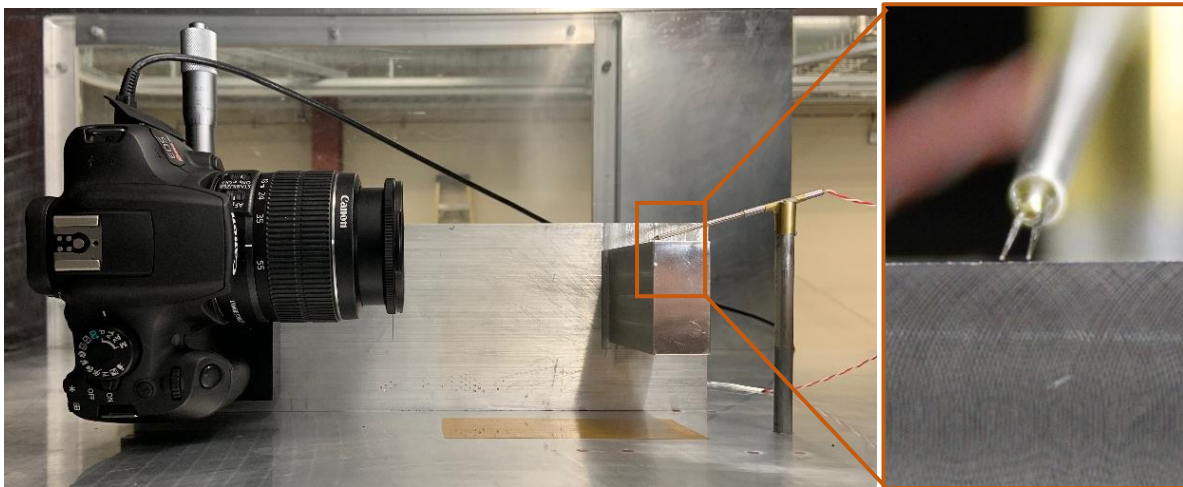


## Hot-Wire Measurements

### Data Acquisition

Boundary layer mean velocity and turbulent stress profiles were taken on the boundary layer development plate and sidewalls using hot-wire anemometry. An A.A. Lab Systems AN-1003 anemometer and a conventional straight sensor probe (Auspex type AHWU-100) were used for the boundary layer surveys. The probe wire was made of 5  $\mu\text{m}$  diameter tungsten with a length of 1.78 mm (0.07 in). The data were acquired at 10 kHz for 20 seconds per point with a 10 kHz low pass filter being used before digitizing the signal with a NI USB 6343 DAQ. An overheat ratio,  $a_r$ , of 2.0 was used with a signal gain of 4.0. Traversing of each profile was achieved with a DC stepper motor with a step size of 0.0127 mm (0.0005 in) per step. Each profile consisted of 48 points with the smallest step increment employed being 0.0254 mm (0.001 in). In order to reduce heat transfer from the wire to the plate when the wire was close to the wall, 0.05 mm (0.002 in) Kapton tape was placed on the surface where each profile was taken.

Alignment of the hot wire probe off the surface was done using a custom camera alignment device. The device consisted of a horizontally mounted camera pointed at the upper edge of a machined aluminum block of known height off the surface. To align the hot-wire, the probe was first traversed up and the camera device positioned underneath the wire. Then both the traverse and camera could be remotely controlled from the computer to precisely lower the hot-wire just over the edge of the block. Once satisfactorily aligned, the camera device could be removed, and the probe finally lowered to its starting location just above the surface. This was done by subtracting the aluminum block offset height (3.345 in  $\pm$  0.001 in) and adding in the Kapton thickness (0.004 in with adhesive) and the desired starting height off the surface (typically 0.002 - 0.010 in).



*Figure 1 Photograph of custom camera alignment device used to determine and align the hot-wire's position above the surface.*

Calibration of the hot-wire was done in situ in the wind tunnel freestream and used the installed pitot tube and Setra pressure transducers used for setting the wind tunnel freestream speed. The Mach 0.6 wind tunnel uses two Setra Model 270 absolute pressure transducers, to measure local static and total pressures respectively, each with a range of 600-1100 HPa and an

accuracy of 0.05% of full scale. Calibrations were done each day of testing and for each separation case. A series of 13 or 14 Mach numbers,  $M_i$ , ranging from 0 to 0.217 or 0.233 were run and the anemometer output voltages,  $E_i$ , recorded along with the ambient fluid temperatures,  $T_i$ . Here the subscript ‘ $i$ ’ is used to denote the calibration points. The calibration points were then converted from Mach number to velocity as follows:

$$U_i = M_i \sqrt{\gamma R T_i} \quad (1)$$

where  $U_i$  is the calibration velocity,  $\gamma$  is the specific heat ratio (taken as 1.4 for air), and  $R$  is the gas constant for air (taken as 287.05 J/(kg·K)). The acquired voltages,  $E_i$ , were corrected for temperature variation to a reference temperature,  $T_r$ , as follows:

$$E_{i,r} = E_i \left[ \frac{T_{wc} - T_r}{T_{wc} - T_i} \right]^{\frac{1}{2}} \quad (2)$$

where  $E_{i,r}$  is the corrected calibration wire voltage at the reference condition,  $T_r$  is the ambient fluid temperature at the reference condition (taken as room temperature 23 °C), and  $T_{wc}$  is the wire temperature defined as follows:

$$T_{wc} = T_i + \frac{a_r - 1}{\alpha_{20}} \quad (3)$$

where  $a_r$  is the overheat ratio  $a_r = R_w/R_a$ , and  $\alpha_{20}$  is the temperature coefficient of resistivity measured at 20 °C (for Tungsten wire  $\alpha_{20} = 0.0036$  °C<sup>-1</sup>). These corrected voltage,  $E_{i,r}$ , and velocity,  $U_i$ , data were then used to generate a calibration plot and the data were fit to a 7th order polynomial yielding voltage as a function of velocity defined as:

$$E(U) = p_1 U^7 + p_2 U^6 + p_3 U^5 + p_4 U^4 + p_5 U^3 + p_6 U^2 + p_7 U + p_8 \quad (4)$$

where  $E = f(U)$  (given by eqn. 4) and the inverse of this equation will be referred to as  $U = g(E)$ . A typical calibration curve is shown below along with the temperature variation. Note that while the temperature drops for the low velocity calibration points, this part of the calibration region is not used as the measured velocity of the boundary layer profiles does not fall below 20 m/s.

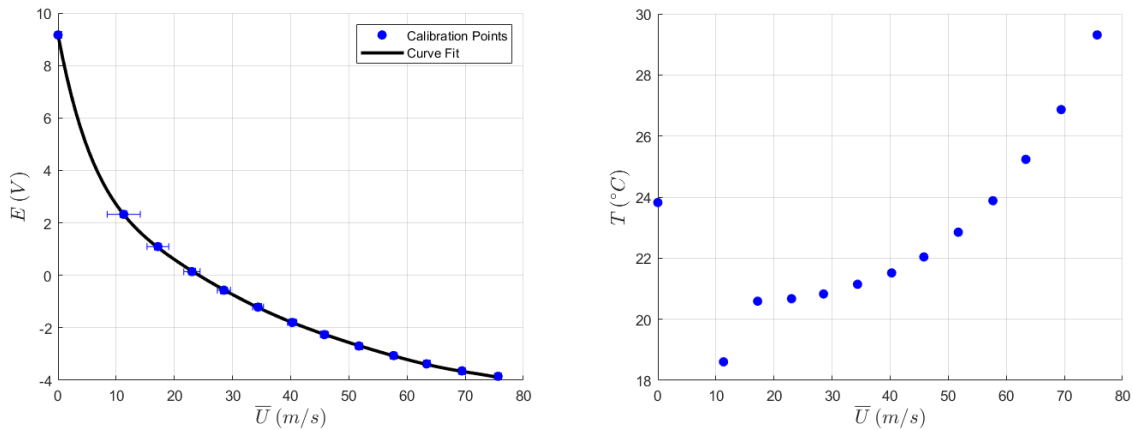


Figure 2 Typical hot-wire calibration curve with voltage (left) and temperature (right) as functions of velocity. Note that confidence intervals are included in the voltage plot and are due to the calibration uncertainty.

Each profile measurement was started with the probe just off the surface (estimated at 0.05 - 0.254 mm) and traversing wall-normal into the freestream. For separation Case A there was very little temperature variation during the extent of the run, typically 1-2 °C, however for Cases B and C the temperature variation became more significant with the variation approaching 10 °C. To correct for temperature effects, the temperature,  $T_a$ , was recorded for each profile. This was done via digital data acquisition for Case B; however, for Cases A and C only manual recording of temperature was done. The hot-wire voltage was corrected to the reference temperature condition using equation (2) applied as:

$$E_{w,r} = E_w \left[ \frac{T_w - T_r}{T_w - T_a} \right]^{\frac{1}{2}} \quad (5)$$

where  $E_w$  is the recorded probe voltage,  $E_{w,r}$  is the wire voltage corrected to the reference condition, and  $T_w$  is the wire temperature defined as follows:

$$T_w = T_a + \frac{a_0 - 1}{\alpha_{20}} \quad (6)$$

The corrected voltage for each data point,  $E_{w,r,j}$ , was then inserted into equation (4) and the equation solved implicitly for velocity,  $u_j$ , via a bisection method. This process was repeated for each data point at each location in the profile. Using the velocity time series, the mean velocity for each location was calculated as follows:

$$\bar{U} = \frac{\sum_{j=1}^N u_j}{N} \quad (7)$$

where  $u_j$  is the instantaneous velocity measurement and  $N$  is the number of samples. The variance was calculated as follows:

$$\overline{u'^2} = \frac{\sum_{j=1}^N |u_j - \bar{U}|^2}{N-1} \quad (8)$$

Sample plots of the mean and variance are shown below.

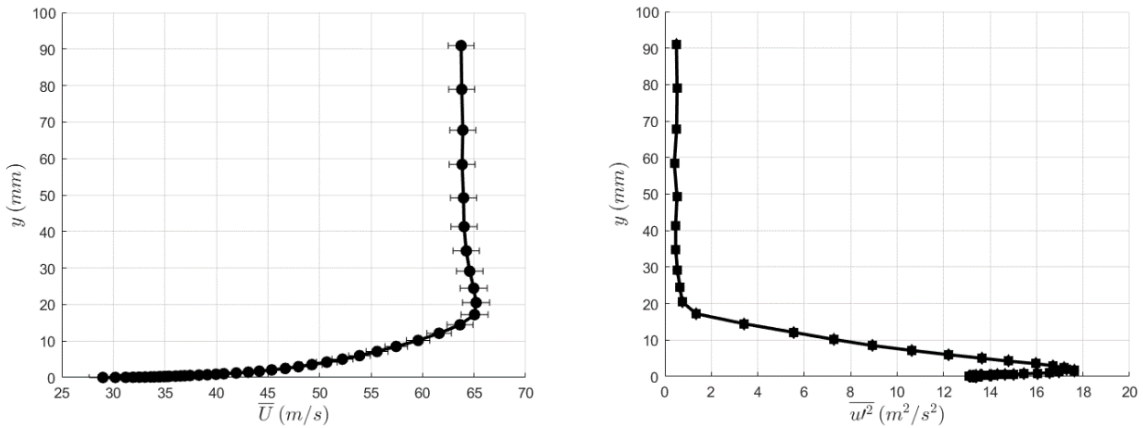


Figure 3 Typical mean velocity (left) and turbulence stress (right) profiles plotted with confidence intervals. These profiles are for Case B with the origin of the profile located at  $(X, Y, Z) = (-0.678, 0.600, 0.457)$ .

## Uncertainty Analysis

The uncertainty analysis procedure followed the general guidelines laid out in the ASME PTC 19.1-2005 Test Uncertainty manual [1] as well as a Dantec hot-wire measurement guide [2]. The combined standard uncertainty of  $U$  is a combination of the random uncertainty,  $s_U$ , and the systematic standard uncertainty,  $b_U$ .

$$u_U = [b_U^2 + s_U^2]^{\frac{1}{2}} \quad (9)$$

The random uncertainty,  $s_U$ , is related to the variance as follows:

$$s_U = \sqrt{\frac{u'^2}{N}} \quad (10)$$

where  $N$  is the number of samples. The overall systematic standard uncertainty is the geometric sum of the individual systematic uncertainties written as:

$$b_U = \left[ \left( \frac{1}{k_\theta} b_\theta \right)^2 + \left( \frac{1}{k_{fit}} b_{fit} \right)^2 + \left( \frac{1}{k_{cal}} b_{cal} \right)^2 + \left( \frac{1}{k_P} b_P \right)^2 + \left( \frac{1}{k_T} b_T \right)^2 + \left( \frac{1}{k_{A/D}} b_{A/D} \right)^2 + \left( \frac{1}{k_D} b_D \right)^2 \right]^{\frac{1}{2}} \quad (11)$$

where  $k_i$  is the coverage factor of the input variance. The systematic uncertainty of the probe angular alignment was estimated using:

$$b_\theta = U(1 - \cos(\theta)) \quad (12)$$

where  $\theta$  is the probe angle with respect to freestream flow. Here,  $\theta$  is estimated to be aligned within  $\pm 3^\circ$ . Since the calibration curve fit implicitly defines  $U(E)$  calculating the systematic uncertainty in the fit required a backward approach as follows:

$$b_{fit} = \frac{b_E}{\frac{\partial E}{\partial U}} \quad (13)$$

where  $b_E$  is the estimated standard error in the voltage produced by using the curve fit for the velocity  $U$  (provided by using the polyval command in MATLAB) and  $\frac{\partial E}{\partial U}$  was calculated using equation (4).

The uncertainty in the calibration,  $b_{cal}$ , is a combination of two primary factors, 1) the accuracy with which the selected calibration flow speeds,  $M_i$  or  $U_i$ , are known, and 2) the deviation of flow from the pitot probe location to the hot-wire probe location during the calibration process, i.e. the freestream flow uniformity. The calibration speeds were set by the wind tunnel controls and are measured by the two Setra pressure transducers. The uncertainty of the flow speeds is calculated from pressure via Bernoulli's equation and from the definition of Mach number equation (14) as follows:

$$M = \sqrt{\frac{2(P_T - P_S)}{\gamma P_S}} \quad (14)$$

where  $P_T$  and  $P_S$  are the local total and static pressure respectively, each measured with a Setra Model 270. The sensitivities of  $M$  with respect to each of the dependent values were obtained by partial differentiation.

$$\frac{\partial M}{\partial P_T} = \frac{1}{M\gamma P_S} \quad (15)$$

$$\frac{\partial M}{\partial P_S} = \frac{-P_T}{M\gamma P_S^2} \quad (16)$$

This gives the uncertainty of the calibration Mach numbers,  $b_{M_{cal}}$  as:

$$b_{M_{cal}} = \left[ \left( \frac{\partial M}{\partial P_T} b_{P_T} \right)^2 + \left( \frac{\partial M}{\partial P_S} b_{P_S} \right)^2 \right]^{\frac{1}{2}} \quad (17)$$

where  $b_{P_T}$  and  $b_{P_S}$  are the uncertainties of the Setra pressure transducers given as 25 Pa. Using this information, the uncertainty in the calibration velocities can then be calculated using equations (17) and (1) as follows:

$$b_{U_{cal}} = \left[ \left( \frac{U}{M} b_{M_{cal}} \right)^2 + \left( \frac{U}{2T} \Delta T \right)^2 \right]^{\frac{1}{2}} \quad (18)$$

where  $\Delta T$  is the uncertainty of the temperature measurements taken as 2 °C. An example of the uncertainty in the calibration velocities is shown in the calibration plot, Figure 2. This uncertainty in the calibration velocity at a given voltage is equivalent to the uncertainty in the flow measurement for the same voltage. The uncertainty in the freestream flow uniformity from the hot-wire location to the pitot tube is likely to be significant, as the freestream velocity appears to vary location to location; however, this uncertainty has not been systematically addressed, hence it will not be considered here. If included, it would be geometrically added to the uncertainty in the calibration velocity as follows:

$$b_{cal} = \left[ (b_{U_{cal}})^2 + (b_{U_{uniformity}})^2 \right]^{\frac{1}{2}} \quad (19)$$

Changes in ambient pressure also produce an uncertainty in the result through their influence on density. Since the calibration velocity actually represents a change in mass flux,  $\rho U$ , the density enters the calibration equation. Hence, the calibration equation could be written as:

$$E(\rho, U) = f(\rho U) \quad (20)$$

The uncertainty caused by changes in ambient pressure can then be written as:

$$b_p = \frac{\partial U}{\partial E} \frac{\partial E}{\partial \rho} \frac{\partial \rho}{\partial P} \Delta P = \frac{U \Delta P}{P} \quad (21)$$

where  $\Delta P$  is the uncertainty or change in the ambient pressure during the calibration and test, estimated as 1 hPa.

While a temperature correction was applied to the calibration and data, there is still uncertainty in the measured temperature, and hence this should be considered as a source of uncertainty. This uncertainty in temperature comes from the fact that the hot-wire voltage is directly related to the heat transfer. To account for this, the voltage-velocity relation is first written in a form relating it to the convective heat transfer.

$$E(\rho, U, T_a) = (T_w - T_a) * f(\rho U) \quad (22)$$

This form of the equation is then used to determine the uncertainty caused by changes in temperature as:

$$b_T = \frac{\partial U}{\partial E} \frac{\partial E}{\partial T} \Delta T + \frac{\partial U}{\partial E} \frac{\partial E}{\partial \rho} \frac{\partial \rho}{\partial T} \Delta T = \frac{-f(\rho U) \Delta T}{(T_w - T_a) * f'(\rho U) \rho} + \frac{-U \Delta T}{T} \quad (23)$$

where the first term is due to convective heat transfer and the second term changes in density caused by temperature.

The uncertainty in the analog to digital conversion can be calculated as follows:

$$b_{A/D} = \frac{E_{AD}}{2^n} \frac{\partial U}{\partial E} \quad (24)$$

where  $E_{AD}$  is the A/D board input range taken as 20 V, and  $n$  is the resolution in bits taken as 16. Of the uncertainty sources examined, this one is the smallest in magnitude and could easily be neglected without changing the overall uncertainty result.

Another systematic uncertainty that arises is a drift in the anemometer voltage as the probe approaches the surface. This can be seen by taking a data set profile with no air flow, recording the voltages, and then running them through the calibration curve fit equation to give velocities. With no air flow the voltage should yield a velocity near zero, with only small deviations due to normal air circulation in the room/wind tunnel. What is seen, however, is that near the surface the indicated velocity is not zero and instead deviates substantially, as shown in right hand Figure 4. Once the probe is about  $y_{off} = 1.4$  mm off the surface, this variation is gone and only the expected small deviations remain with the voltage being roughly  $E_{cal} = E(0)$ .

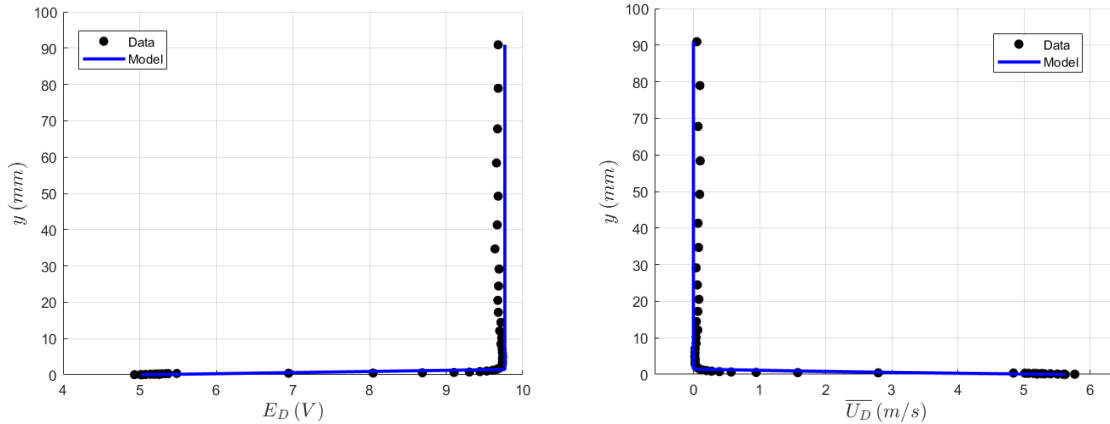


Figure 4 Plot of drift voltage (left) and drift velocity (right) as functions of wall-normal height for a test with no air flow, i.e.  $M = 0$ . Note that near the surface the voltage (left) drifts causing an “artificial” velocity (right) to appear.

This near wall effect could be due to heat transfer and should be included in the uncertainty of the measurements. The drift in voltage was not nearly this substantial in most of the cases, so this example should be treated as the extreme case; however, the trend was the same. To account for this effect, instead of taking a no-flow profile before each test, the drift in voltage was recorded at the first point near the wall,  $E_{wall}$ , before the test was started. This was then fit to a linear function of voltage vs wall normal location that only extended  $y_{off} = 1.4$  mm off the surface with the remaining drift voltage being set to  $E_{cal}$ . In equation form this is written as:

$$E_D = \frac{E_{cal} - E_{wall}}{y_{off}} y + E_{wall} \quad (25)$$

where  $E_D$  is the drift voltage and is a function of the wall-normal location. The uncertainty that this produces in the velocity,  $b_D$ , is calculated by inputting the drift voltage into the calibration curve fit equation (4) and solving by the bisection method to yield the drift velocity. This can be written as follows:

$$b_D = g(E_D) \quad (26)$$

This model is also shown in Figure 4 and compares quite well to the observed data. Again, most profiles did not drift as far as 5 V, and were instead in the 7-9 V range.

A list of the uncertainty sources just discussed, and their estimated magnitudes, are shown in Table 5. It should also be pointed out what sources of uncertainty were not considered here. As mentioned, the uniformity of the freestream flow is not known. Additionally, the effects of spatial averaging over the span of the hot-wire length likely influences the shape and magnitude of the variance profiles. This can be seen when the variance is written in the form of turbulence intensity. Hutchins et al. [3] provide a likely explanation for this phenomena in the attenuation of small scales due to a large viscous scaled wire length,  $l^+$ , approximately 271 here. For further discussion see Hutchins et al. [3].

Table 1 Systematic uncertainty sources and estimate values for the conducted hot-wire anemometry profiles.

Uncertainty Source	Estimated Uncertainty	Coverage Factor	Remarks
Probe angular alignment: $b_\theta$	$\pm 0.14$ % of $U$	$\sqrt{3}$	Estimated uncertainty in alignment with streamwise flow direction.
Curve fit: $b_{fit}$	$\pm 1$ % of $U$	2	Estimated by using the standard error of the curve fit $E = f(U)$
Calibration: $b_{cal}$	$\pm 1$ % to $\pm 4$ % of $U$	2	Only includes the uncertainty of the calibration points, not the freestream flow non-uniformity.
Temperature: $b_T$	$\pm 1$ % of $U$	$\sqrt{3}$	Estimated based off thermocouple uncertainty of 2°C.
Ambient Pressure: $b_p$	$\pm 0.1$ % of $U$	$\sqrt{3}$	Estimated based off a 1 hPa change in ambient pressure during the calibration and test.
A/D Resolution: $b_{A/D}$	$\pm 0.01$ % of $U$	$\sqrt{3}$	For the NI DAQ with 16 bits of resolution and 20 V input range.
Voltage Drift: $b_D$	$\pm 0$ % to $\pm 5$ % of $U$	$\sqrt{3}$	This uncertainty is only substantial near the surface and in most cases peaks around 2% of $U$ .

An example of the elemental uncertainty of each of the systematic uncertainty components and the random uncertainty are shown as a function of the wall-normal profile point in the bar graph in Figure 5. Here, the sum of each element is scaled to equal 100% to highlight the relative magnitude of each uncertainty source and the profile point starts at the wall (point 1) and continues into the freestream (point 48). In general, the uncertainties due to calibration, temperature, curve fit, and voltage drift are the most significant, with substantial variation across the boundary layer profile.



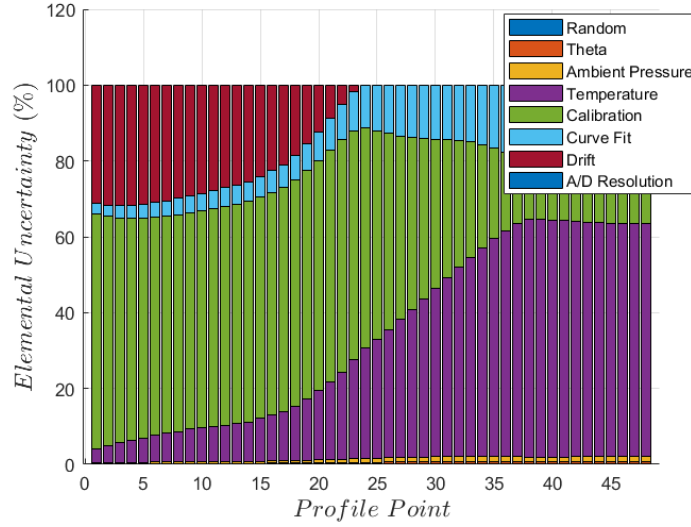


Figure 5 Plot of the relative uncertainty due to each of the sources discussed as a function of the boundary layer height. Here the uncertainty of each source is written as a percentage of the total uncertainty at each point. Note that the profile point starts just off the surface, Profile Point 1, and continues into the freestream, Profile Point 48.

The combined standard uncertainty was given in equation (9) and is a combination of the random uncertainty and the systematic standard uncertainty. The expanded uncertainty is the combined standard uncertainty multiplied by the Student's t-table value,  $t_{v,p}$  where  $v$  is  $N - 1$  and  $p$  is the selected confidence interval. At 20:1 odds or  $p = 95\%$  confidence and assuming a large sample size,  $t_{v,p} = 1.96$ . Using this analysis, the true value is expected to lie within:

$$U \pm t_{v,p}u_U \quad (27)$$

where  $t_{v,p}u_U$  is the expanded uncertainty or simply the uncertainty of the quantity.

The uncertainty considered thus far is with respect to the mean velocity,  $U$ . It is assumed that the systematic uncertainties examined only effect the mean not the variance. Thus, the uncertainty of the variance is solely a function of the variance, the kurtosis, and the number of samples and can be written as:

$$u_{u'^2} = \sqrt{\frac{u'^4 - u'^2}{N}} \quad (28)$$

This yields the expanded uncertainty as:

$$\overline{u'^2} \pm t_{v,p}u_{u'^2} \quad (29)$$

## References

- [1] *ASME PTC 19.1 - 2005 Test Uncertainty*. ASME, 2005.
- [2] Finn E. Jorgensen. How to Measure Turbulence with Hot-Wire Anemometers - a Practical Guide.
- [3] Hutchins, N., Nickels, T. B., Marusic, I., and Chong, M. S. "Hot-Wire Spatial Resolution Issues in Wall-Bounded Turbulence | Journal of Fluid Mechanics | Cambridge Core." *Journal of Fluid Mechanics*, Vol. 635, 2009, pp. 103–136.